An Assessment of Multi-copter Noise in Edgewise Flight

Brendan Smith
PhD Student

Dr. Farhan Gandhi
Redfern Chair, Director

Center for Mobility with Vertical Lift (MOVE)
Rensselaer Polytechnic Institute
Troy, New York, United States

Dr. Anastasios Lyrintzis
Distinguished Professor & Chair

Department of Aerospace Engineering
Embry-Riddle Aeronautical University
Daytona Beach, Florida, United States

ABSTRACT

This study examines the acoustic behavior in forward speeds of 0, 15, 30, and 60 knots of manned-size, multi-rotor, eVTOL aircraft in quadcopter, hexacopter, and octocopter configurations. The rotors are assumed to have constant RPM and are controlled through collective pitch, with orthogonal phasing between rotors. All configurations share the same disk loading and hover tip Mach, with the rotor radius decreasing and the RPM increasing as the number of rotors increase. The simulations use the Rensselaer Multicopter Analysis Code (RMAC) for the aerodynamic loads coupled with the PSU-WOPWOP code for noise predictions at an observer hemisphere. From the results, it is shown that at higher forward flight speeds, where loading noise becomes more dominant, high elevation angles (below the vehicle) show peak noise for all configurations. Asymmetry in the number of outside advancing blades, such as on the plus quadcopter, causes higher noise levels for the left (advancing) side. In-plane directivity patterns that show large decreases due to signal cancellations in inter-boom noise are shown to progressively diminish at larger forward speeds, with lower reductions for the hexacopter and octocopter configurations. The total acoustic radiated power is also compared with the single rotor for all multicopter configurations. The comparison shows that the acoustic power versus the single rotor power is decreasing as we increase the number of rotors or the forward speed.

1. INTRODUCTION

Due to the evolution of electric batteries and electric motors at larger scales, interest in developing multi-rotor electric Vertical Takeoff and Landing (eVTOL) vehicles has risen in recent years. Although the concept is not new, having been available on a small scale commercially for some time, there is now a thrust for larger, *manned-size* eVTOL aircraft to support the vision of Urban Air Mobility (UAM) as suggested, for example, by the Uber Elevate Program (Ref. 1) and the NASA UAM Grand Challenge (Ref. 2). The vision put forward by these programs includes ubiquitous use of these manned-size eVTOL aircraft for operations such as transportation of goods and persons across various urban and suburban landscapes. This vision, however, requires overcoming many large technical and logistical challenges.

A key technical challenge is the noise generated by eVTOL aircraft operating in these areas of high population density, and its impact on community acceptance. Over the past several decades, a lot of work has been done to develop a good understanding of the aeroacoustic characteristics of conventional helicopters. Ref. 3 details the key noise sources of thickness noise, loading noise, high-speed impulsive noise, blade-vortex interaction noise, and broadband noise on conventional helicopters and discusses their relative importance. However, for multi-rotor eVTOL, there is no similar level of understanding as of yet.

As a result, many research groups have undertaken significant efforts to improve the understanding of eVTOL noise. NASA Langley Research Center (LaRC) and other academic research groups have generated a large body of work on experimental measurements and corresponding simulations for small, fixed-pitch, variable RPM rotors and their assemblies (Refs. 4-11). These studies have examined several issues including the relative importance of noise sources, rotor-airframe interaction effects, the importance of broadband noise, and the effects of phase synchronization between rotors.

There have been several simulation studies that focus on the larger multi-rotor aircraft supporting the UAM vision, e. g. Quackenbush et al., (Ref. 12) and Jia and Lee (Ref. 13). Significant attention has been devoted to broadband noise for variable-RPM eVTOL rotors (Refs. 14, 15) which has been shown to be a more significant noise source than on traditional helicopters (Refs. 11, 16). Another important area is the aeroacoustic implications of propeller-wing, -body, -duct, and -boom interactions typically encountered on eVTOL aircrafts (Refs. 17, 18). Along with these propeller interactions, there are also rotor-rotor aerodynamic interactions that need to be accounted for. Studies have been conducted using CFD and

Submitted to Vertical Flight Society's 77th Annual Forum & Technology Display, West Palm Beach, Florida, May 11-13, 2021

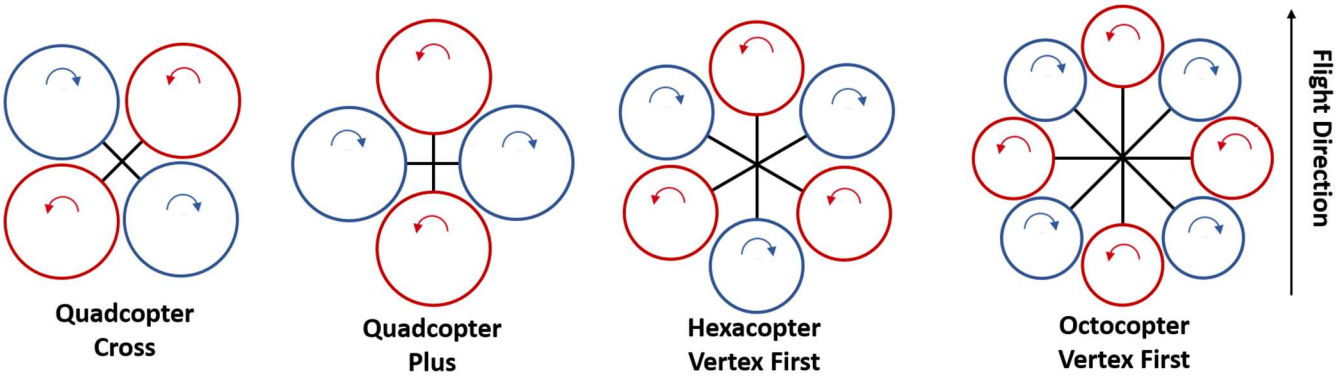

Figure 1: Multi-copter orientations

Vortex Particle Methods (VPM) to examine these effects for side-by-side configurations and stacked configurations (Refs. 19-21).

Other factors are also being considered in eVTOL aircraft development that have implications on the aeroacoustics. While all small multi-copters are controlled through variation in RPM, there are recent studies that suggest that as rotor diameter increases, variable-RPM control alone may not meet the handling quality requirements set forth, specifically in disturbance rejection characteristics (Refs. 22-25). One solution to solve this challenge is collective pitch control on individual rotors, with one design including this feature being Joby Aviation's 4-passenger S4 aircraft (Ref. 26). Collective-pitch control allows for potential phase synchronization between rotors, which has already been explored for vibration reduction on eVTOL aircraft in Refs. 27 and 28.

Our study examines the aeroacoustic characteristics of UAM-scale, multi-rotor eVTOL aircraft in forward flight, specifically examining the effects of number of rotors and changes in disk loading on the noise levels and the radiated acoustic power.

2. ANALYSIS

The aerodynamic loads for each of the multi-rotor configurations considered are generated using the Rensselaer Multicopter Analysis Code (RMAC), a physics-based comprehensive and flight-simulation analysis tool (Ref. 29). RMAC uses blade-element-theory, in conjunction with a 10-state Peters-He finite-state dynamic wake model to calculate the blade sectional aerodynamic loads which can be integrated along the span and around the azimuth to obtain the rotor loads.

Three multi-copter configurations are considered in this study: a quadcopter, hexacopter, and octocopter, as well as a single rotor. All configurations have the same equivalent disk area. The multi-copters are evaluated in cruise, and as such orientation of the rotors in reference to the flight direction is important, which are shown in Figure 1. The quadcopter is considered in two different orientations: cross, which sits two rotors in front and two rotors at the rear, and plus which sits one rotor in front, two in the middle, and one at the rear. The hexacopter and octocopter are considered at one orientation, vertex first, meaning the multi-copter is flying with a single rotor in front and a single rotor at the rear, with the remaining rotors in pairs. The starting phase of the rotors is set to "orthogonal", in which neighboring rotors are completely out of phase, as shown for the cross quadcopter in Figure 2.

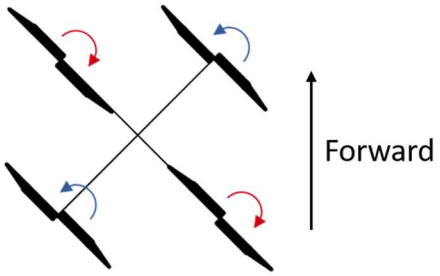

Figure 2: Cross quadcopter configuration with orthogonal phasing

All configurations are examined in hover and at 15, 30, and 60 knots of nose-level forward flight. To maintain thrust, the root pitch of the rotors is trimmed to maintain balance, using the assumption that a propulsion device is being used to achieve adequate speed. This means the root pitch of rotors may differ, but the RPM is always help constant which maintains the orthogonal phasing.

To enable comparison between the multi-copters, parameters such as disk loading, number of blades, blade twist rate, and blade taper ratio are held constant. These values are given in Table 1. The airfoils used are constant, with a linear

Table 1: Rotor Parameters

Parameter	Value
Disk Loading	6 lb/ft^2
Number of Blades	2
Twist Rate	-12° per span
Taper Ratio	0.75

blend of a NACA 2412 at the root to a Clark Y at the tip. To maintain constant disk area, as the number of rotors increases the radius of each rotor is decreased. The length of the booms for each multi-copter is always such that there is a clearance between adjacent rotors of 10% of the rotor's radius. To preserve the hover tip Mach number between multi-copters (nominally 0.51), the rotor RPM is increased as the number of rotors increase. The values for the rotor radius and rotor RPM of each multi-copter configuration, as well as an equivalent single rotor, are given in Table 2.

The blade loads for the rotors are provided as inputs to PSU-WOPWOP (Ref. 30), an acoustic propagation code based on the numerical implementation of Farassat's Formulation 1A of the Ffowcs Williams and Hawkings (FW-H) equation. The RMAC loads are provided as chordwise compact loads, with acoustic analysis considering only tonal noise from thickness and loading noise sources. Observers are arranged in a 100 ft radius hemisphere (12.5 times the equivalent single rotor radius, denoted as R_o) in 5 deg increments in azimuth and elevation angle, shown in Figure 3. At each observer, the Overall Sound Pressure Level (OASPL) in dB and dBA is calculated from the acoustic time pressure history.

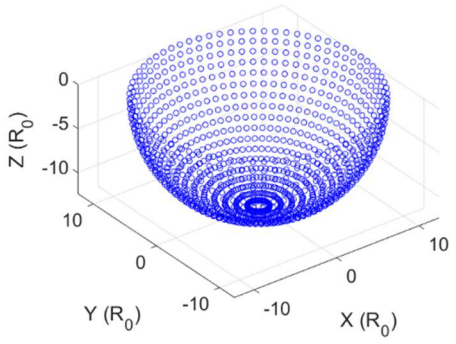

Figure 3: 100-foot radius observer hemisphere

Table 2: Multi-copter and single rotor radius and RPM

Platform	Radius	RPM
Single Rotor	8 ft (2.428 m)	685.5
Quadcopter	4 ft (1.219 m)	1371
Hexacopter	3.23 ft (0.995 m)	1679
Octocopter	2.83 ft (0.862 m)	1939

The total acoustic power radiated (PWL) is also calculated for each configuration at different flight speeds over the observer hemisphere. To calculate this, first the sound intensity at each observer is calculated using the acoustic pressure history:

$$I = \frac{p^2}{\rho c} \quad (1)$$

where p^2 is the mean square pressure at the observer, ρ is air density, and c is speed of sound. To obtain the PWL, the sound intensity is integrated over the surface of the observer grid. These values are then normalized with respect to the equivalent single rotor for a given cruise speed using:

$$PWL_{dB} = 10 * \log_{10}\left(\frac{PWL_{multicopter}}{PWL_{equivalent\ single\ rotor}}\right). \quad (2)$$

3. RESULTS

3.1 Single Rotor and Cross-configuration Quadcopter

Figure 4 shows the overall sound pressure level (OASPL) in dB at the hemisphere observer grid for the single rotor at forward flight speeds of 0, 15, 30, and 60 knots. The hover condition shows uniform 84 dB noise. As the rotor increases its forward speed, this uniformity breaks down, with higher noise appearing at higher elevation angles (towards the bottom of the hemisphere) and lower noise showing at elevations close to the plane of the rotor (0°). This is expected as loading noise (propagating at high elevation angles) is increasing in forward speeds due to unsteady forces and dominates the thickness noise (propagating near the plane). The values for peak and low noise also become more different at higher speeds. As previously mentioned, in hover the noise is about 84 dB, but at 60 knots the noise ranges from a max of 99 dB to a minimum of 77 dB. For medium and high elevation

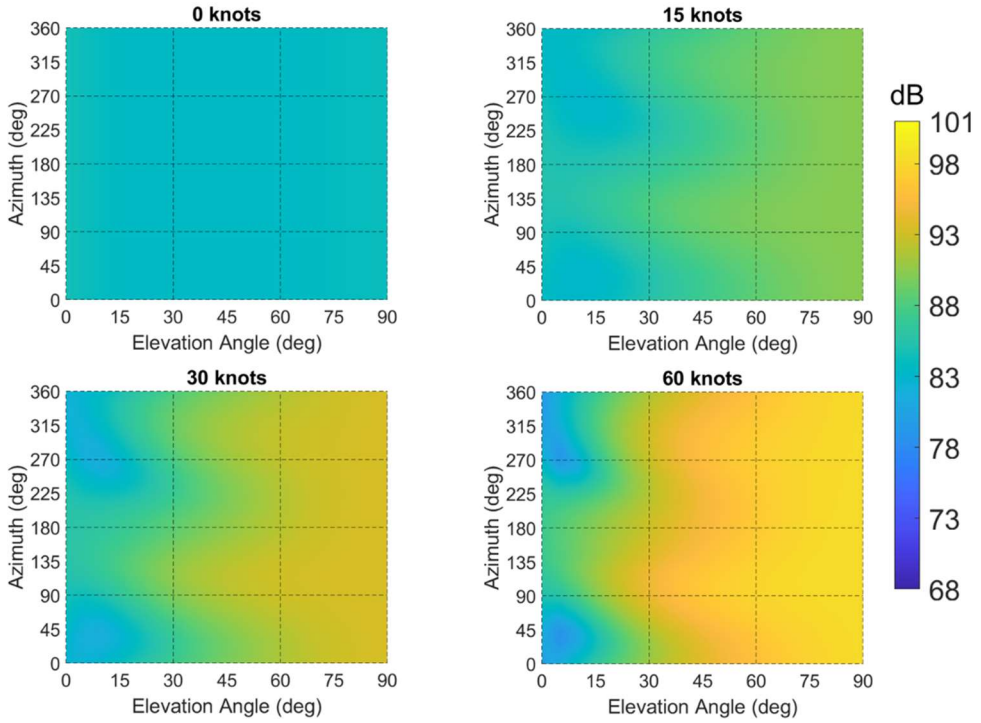

Figure 4: Single rotor for (top left) 0 knots (top right) 15 knots (bottom left) 30 knots (bottom right) 60 knots forward speed

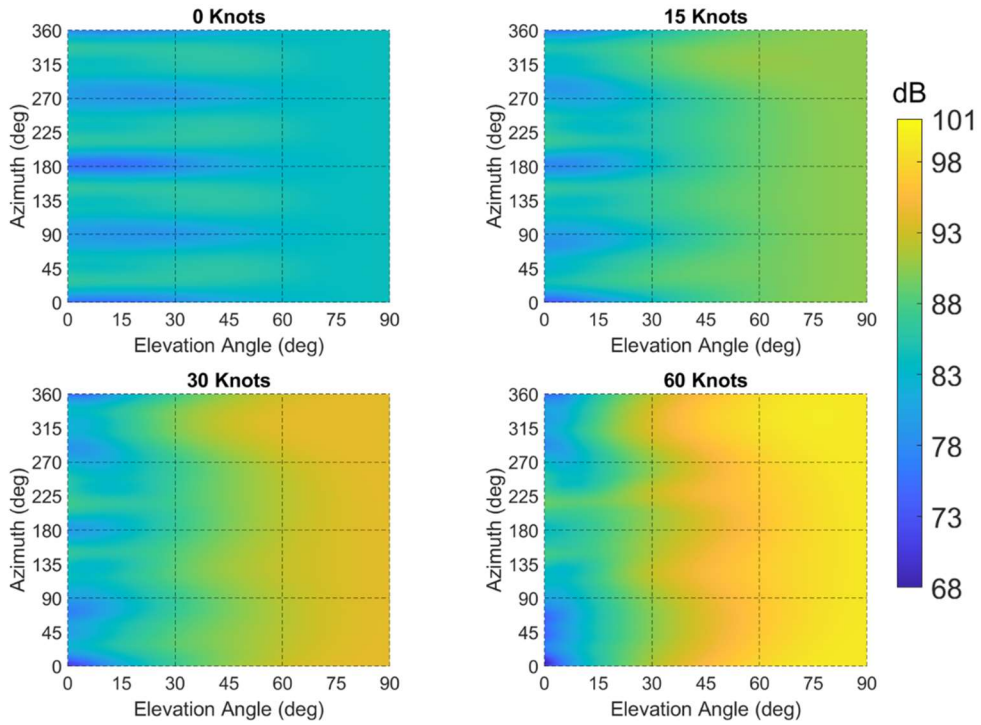

Figure 5: Cross quadcopter for (top left) 0 knots (top right) 15 knots (bottom left) 30 knots (bottom right) 60 knots forward speed

angles, the noise concentrates towards the advancing side of the rotor, (90°) azimuth, where more loading noise is being generated in forward flight speeds.

These trends can be contrasted with the results for the cross-configuration quadcopter given in Figure 5. In hover, as detailed in Ref. 31, at low elevation angles (near rotor plane) deep lows are observed for inter-boom locations (0°, 90°, 180°, 270° azimuth) and peak noise is observed at azimuth angles corresponding to rotor locations. These directivities are due to amplification/cancellation patterns because of the rotor phasing and the differences in the acoustic paths for a given observer. The lows are observable at 15 knots forward flight, but at 30 and 60 knots the lows in front of the vehicle disappear, and like the single rotor the low noise congregates towards the back of the vehicle in-plane. Also, similar to the single rotor, the peak noise increases at forward speeds and concentrates below the vehicle. The values are farthest apart at the fastest speed of 60 knots, with a maximum of 101 dB and a minimum of 60 dB, compared to a spread of 86 dB to 75 dB observed at 0 knots. The amplification/cancellation directivity patterns appearing for the hover condition are reduced by the forward speed and eventually disappear. This is expected if we examine the signals from the four rotors in the rotor plane. For example, if we look at inter-boom locations (e.g. 90°) the signal from the four rotors arrives out of phase (causing cancellations) for hover, but at forward speeds cancellation cannot be achieved as the 4 rotors being at different local azimuth angles, create a different signal for each rotor. This effect is more pronounced at higher forward speeds, eventually breaking down the directivity pattern detected at hover. Furthermore, as we increase the elevation angle the difference in the acoustic paths due to the rotors location and phasing is reduced. Therefore, in moderate and high elevation angles the directivity patterns are much less or not at all detectable.

3.2 Varying Number of Rotors

Now that a baseline comparison has been established between the cross quadcopter and the single rotor, different configurations can be considered. As detailed in the analysis, the plus orientated quadcopter is another possible quadcopter configuration. We will also examine a higher number of rotors, i.e. a hexacopter and octocopter. Figure 6 exhibits the OASPL in dB at the observer hemisphere shown in figure 3 for the aforementioned multi-copters in hover, as also shown and discussed by Smith et al. (Ref. 31)As expected, the plus quadcopter shows the same noise signature as the cross quadcopter, just shifted by 45° azimuth. At elevation angles close to 0° (in-plane), the hexacopter shows areas of low noise every other inter-boom location (90°, 210°, 330° azimuth), and high noise at azimuth angles corresponding to rotor locations. These high noise regions are louder than observed on the quadcopter, which showed a maximum of 86 dB relative to the 90 dB maximum found for the hexacopter. The octocopter shows low noise at every inter-boom location, and high noise at every rotor location at lower elevation angles. The difference between these highs and lows is the largest for any of the multi-copters, with a difference of 16 dB. For all multi-copters, these differences in noise signature are just at low elevation angles. At high elevation angles, where loading noise is the dominant noise source, the OASPL is ~84 dB for all configurations.

Figure 7 shows the OASPL over the observer grid for the multi-copters for forward flight of 15 knots. As with the cross quadcopter, the minimum noise regions at low elevation angles are still visible at forward speed for all the other configurations. However, the regions of high noise are very different between configurations. The cross quadcopter shows the peak noise developing below the vehicle with mostly uniform distribution across azimuth angles, which is not shown for the other multi-copters. For the plus quadcopter, the peak noise develops at medium elevation angles (~30°-60°) and is heavily concentrated on the left side of the vehicle. This concentration on the left side is shown for both the hexacopter and the octocopter as well. They both retain the high and low noise regions exhibited at 0 knots, but the high noise regions on the left side are greater than those exhibited on the right side. This is expected, as in all these three configurations (plus quadcopter, hexacopter, and octocopter) there more rotors on the left side with the advancing side on the outside, whereas on the right side the advancing side is on the inside. This is more evident on the quadcopter plus, where the right rotor advancing side is towards the inside, while the left rotor advancing side is located towards the outside left of the aircraft. Therefore, there is a large asymmetry (between left and right) for this case. However, the quadrotor cross is symmetric between left and right (advancing side is outside for both left and right rotors), and thus creates a relatively symmetric signal, at high elevation angles, when the differences due to rotors location and phasing (apparent in the in-plane signals) diminish as will be also shown in higher speeds later

Figure 8 shows the same OASPL plots, but for 30 knots forward flight. The trends observed for 15 knots continue to be exhibited, but now have become more pronounced. The plus quadcopter no longer exhibits low noise areas in the front for low elevation angles, with the low noise regions concentrating towards the rear of the vehicle as was shown for the cross quadcopter. Again, the louder noise region moves towards the left side of the vehicle at medium elevation angles, with the peak noise of 94 dB exhibited at an azimuth angle of 270° corresponding to a rotor location. This is in contrast to the cross quadcopter, which shows more of an even distribution for louder noise regions. Both the hexacopter and octocopter still exhibit the lower elevation angle directivity that are observed in hover, but peaks towards the rear of the aircraft are stronger than those observed in the front. There is also a left side bias, with the peak noise of 94 dB being

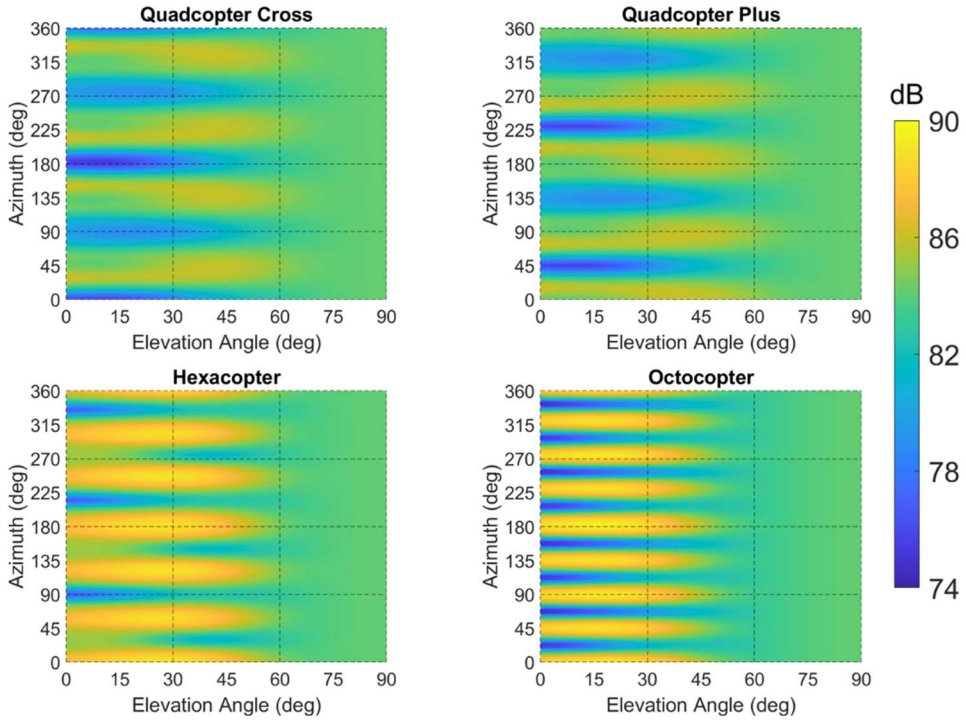

Figure 7: 15 knots forward speed for (top left) cross quadcopter (top right) plus quadcopter (bottom left) hexacopter (bottom right) octocopter

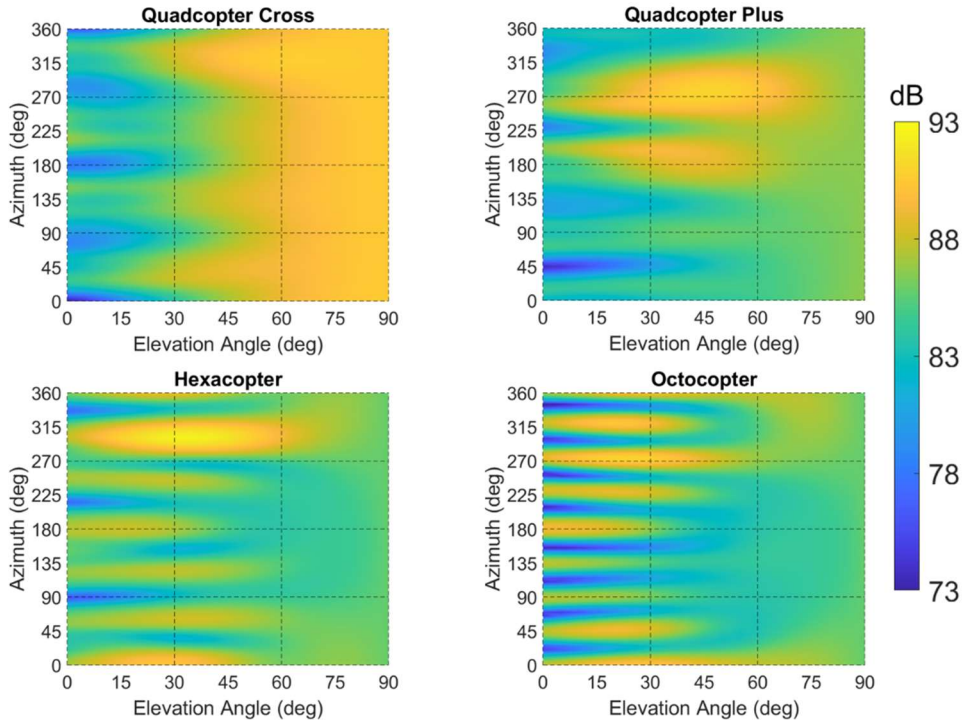

Figure 6: 0 knots forward speed for (top left) cross quadcopter (top right) plus quadcopter (bottom left) hexacopter (bottom right) octocopter

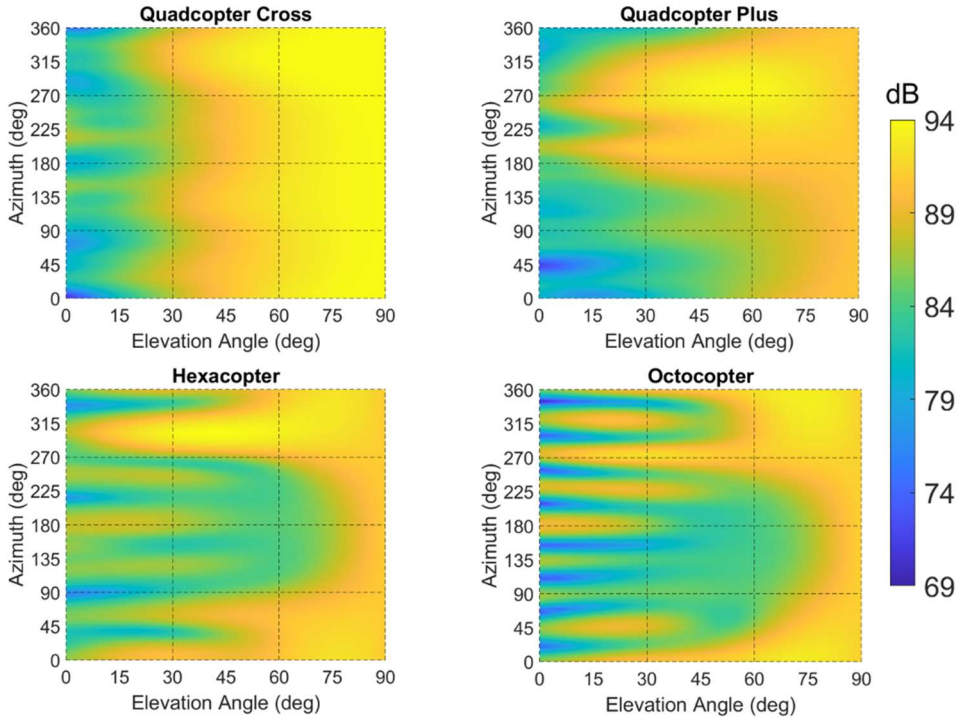

Figure 9: 30 knots forward speed for (top left) cross quadcopter (top right) plus quadcopter (bottom left) hexacopter (bottom right) octocopter

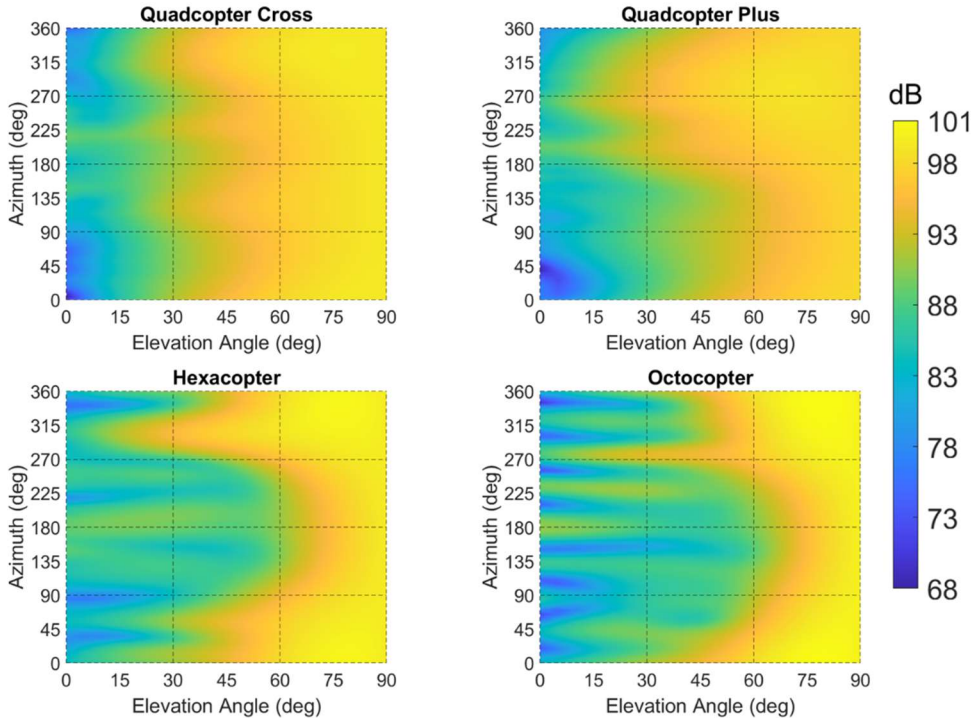

Figure 10: 60 knots forward speed for (top left) cross quadcopter (top right) plus quadcopter (bottom left) hexacopter (bottom right) octocopter

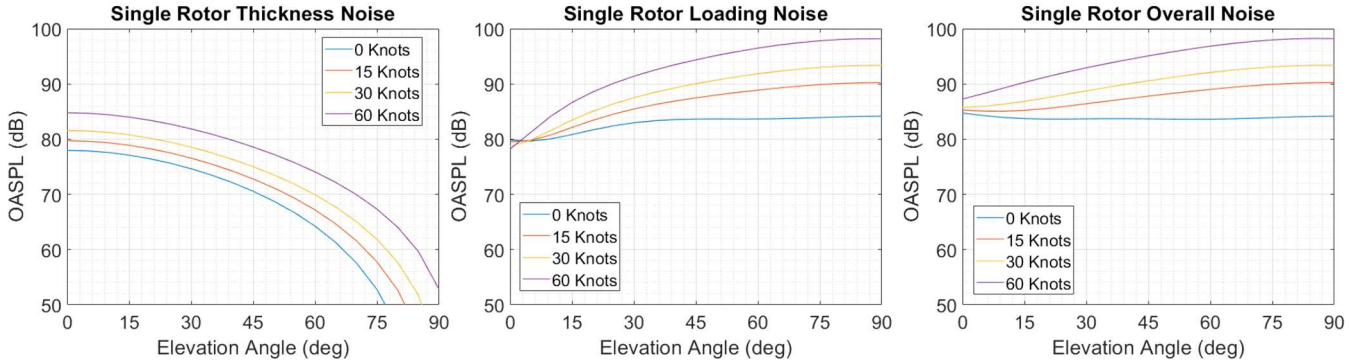

Figure 10: Breakdown of single rotor noise sources for 0, 15, 30, 60 knots forward speed at azimuth angle 180°

exhibited at ~300° azimuth for the hexacopter and the same peak noise for the octocopter being located at 270° azimuth, both being rotor locations. These trends were explained in the previous discussion of the 15 knots case. However, unlike the 15 knots, all configurations now exhibit regions of loud noise at high elevation angles, as loading noise becomes more dominant. This region of loud noise is the largest for the cross quadcopter, and less pronounced for the hexacopter and octocopter.

Figure 9 shows the OASPL in dB at the observer hemisphere for the multi-copters in 60 knots forward flight. The plus quadcopter shows mostly the same as with 30 knots, with peak noise concentrated below the vehicle towards the left side. The lower elevation angle directivity displayed by the hexacopter is less pronounced than in lower flights speeds. This is also true for the octocopter, although the lows at inter-boom locations are still distinct, maintaining a large part of the directivity pattern observed in hover. The largest change for the plus quadcopter, hexacopter, and octocopter comes from the location of the peak noise. While for 0, 15, and 30 knots forward speed the location of peak noise is different in terms of elevation angle, mostly being found in the region of 30°-60°, now the peak noise for all configurations resides below the vehicle (elevation angle 90°).

The general trends can be explained by revisiting the different noise sources, thickness and loading, for the single rotor. Figure 10 gives graphs showing how the different noise sources change with elevation and forward speed for the single rotor, at an azimuth location of 180°. As forward speed increases, loading noise directed at high elevation angles becomes more and more dominant, where the thickness noise is negligible. Thus, when 60 knots is reached, loading noise will be dominant and directed below the vehicle, and thus the high noise region will be found there. Therefore, differences between configurations are found more in the medium to lower elevation angles, which will be quantitatively discussed in the following paragraph(s).

Figure 11 shows polar plots of the in-plane noise in front of the multi-copters, for 0, 15, 30, and 60 knots forward flight speed. A significant difference that is immediately apparent is how the noise directivity of the multi-copters changes with forward speed. Both quadcopters, cross and plus, lose most of the forward directivity that is exhibited in hover, especially the deep lows that are found at inter-boom locations. However, both the hexacopter and the octocopter maintain their directivity, with changes in magnitude but no overall change in shape. A possible explanation is that acoustics paths from different rotors have a smaller difference for the hexacopter and octocopter configurations than for the quadcopter configurations. Therefore, the effects of forward flight (that diminish the amplification cancellation patterns) are lower. Along with the loss of directivity, the quadcopter configurations show larger maximum increase in noise, with an increase of ~8 dB at an azimuth angle of 180° for the cross configuration and 225° for the plus configuration. In terms of averages however, the difference is not so large, with a change in average noise of 2.5 dB for the cross quadcopter and 1.8 dB for the plus quadcopter. The hexacopter exhibits regions of noise increase across the forward portion and noise reduction towards the right. There is a small overall increase in average noise of 0.8 dB between hover and 60 knots forward flight. The octocopter does show some increase along portions of the front half, namely towards the front. But this does not result in any real change in average noise, with only a 0.1 dB average noise increase when moving into 60 knots forward flight. The plus quadcopter, hexacopter, and octocopter all exhibit a reduction in noise towards the right side that is not present of the cross quadcopter. This reduction is 3 dB for the plus quad at ~90° azimuth, 3 dB for the hexacopter at 120° azimuth, and 4 dB for the octocopter at 90° azimuth. Like discussed previously, the right sides for these configurations have rotors with advancing sides inside and thus the effects of forward flight are diminished there. Overall, while slight noise increases are observed, forward flight has less of an effect in-plane than other elevations. This is expected, as the main effect of forward flight is increasing the loading noise.

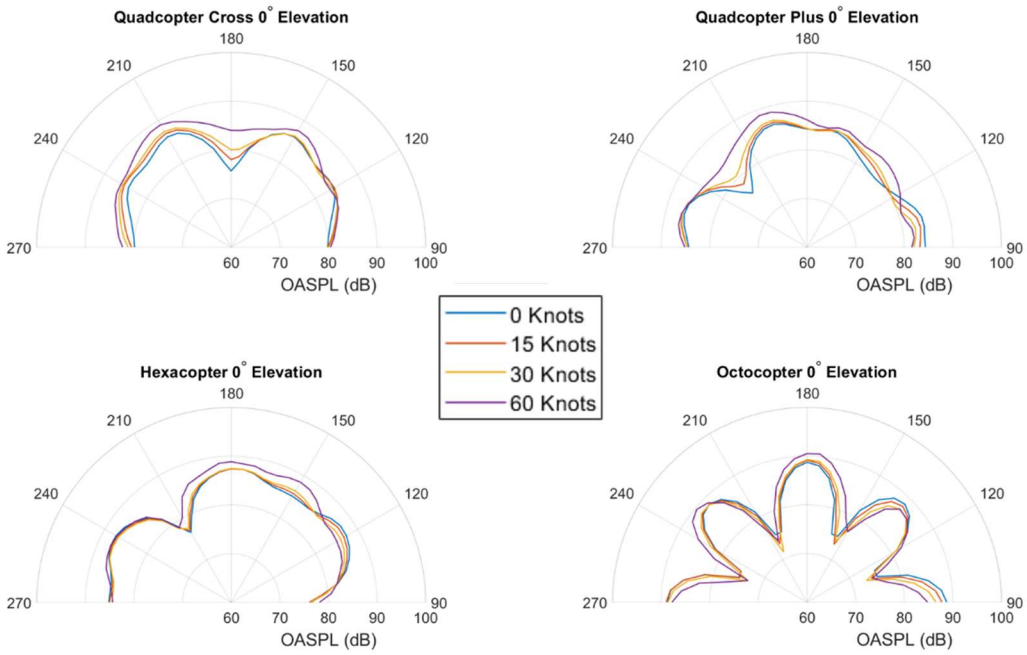

Figure 11: Forward Polar Plot In-Plane (0°) for (top left) cross quadcopter (top right) plus quadcopter (bottom right) hexacopter (bottom left) octocopter

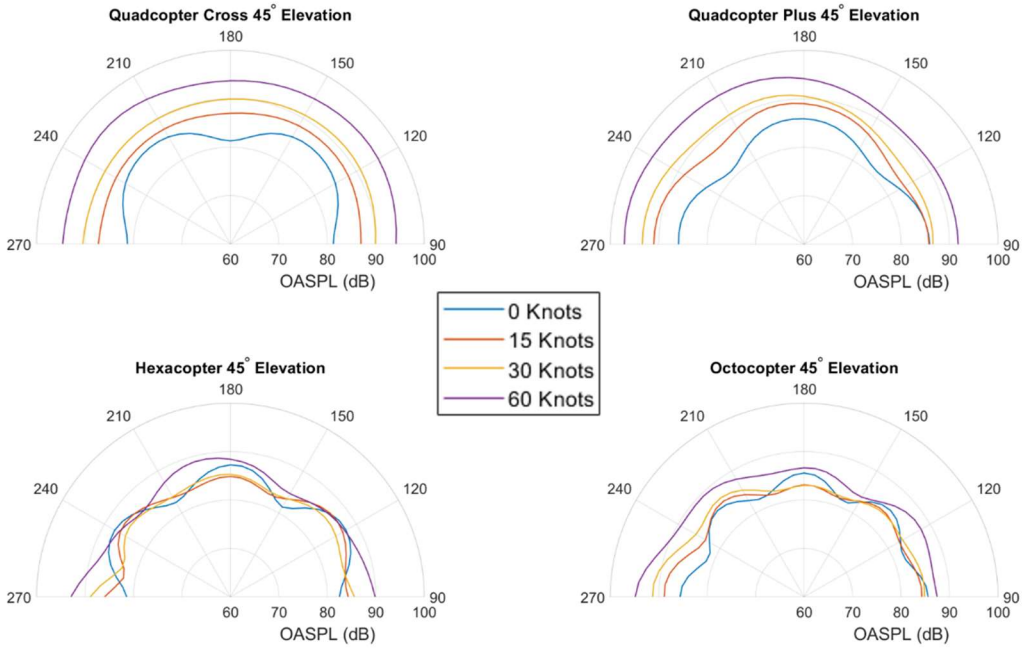

Figure 12: Forward Polar Plot at 45° elevation for (top left) cross quadcopter (top right) plus quadcopter (bottom right) hexacopter (bottom left) octocopter

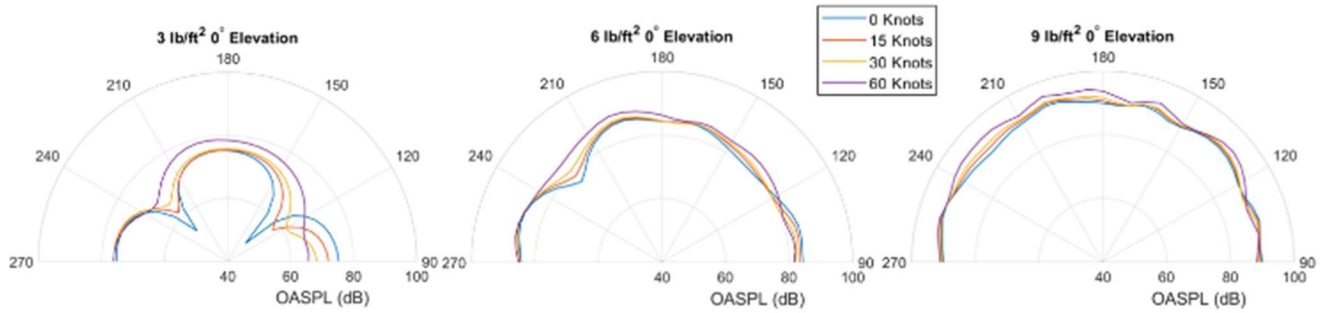

Figure 13: Forward Polar Plot In-Plane (0°) for plus quadcopter with disk loading (left) 3 lb/ft^2 (center) 6 lb/ft^2 (right) 9 lb/ft^2

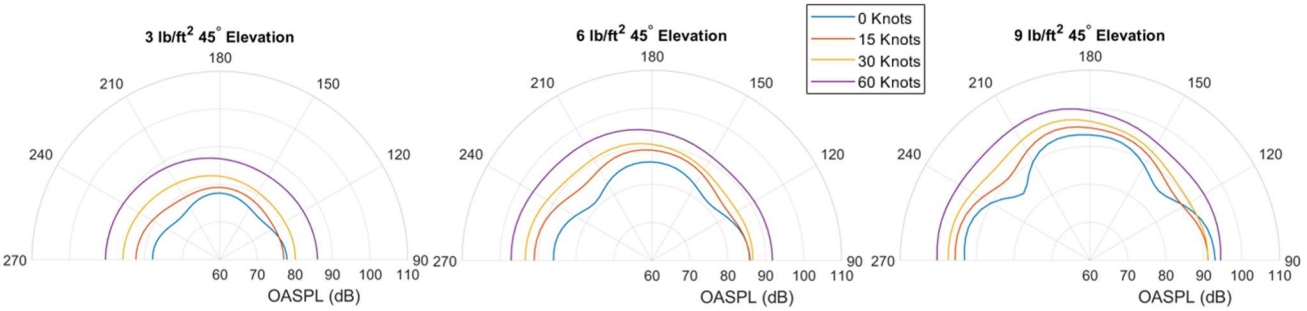

Figure 14: Forward Polar Plot at 45° elevation for plus quadcopter with disk loading (left) 3 lb/ft^2 (center) 6 lb/ft^2 (right) 9 lb/ft^2

This same comparison for the 45° elevation angle is given in Figure 12. As discussed when observing the OASPL over the hemispheres, the directivity is not preserved for any of the multi-copters at higher forward flights speeds for 45° elevation as opposed to results shown for the 0° elevation. As discussed before (near the end of section 3.1), as we increase the elevation angle the difference in the acoustic paths due to the rotors location and phasing is reduced. Thus, at 45° elevation is much less or not at all detectable at high forward speeds. The noise increases are also greater for all configurations, though most evident in the quadcopter, similar to in plane. The cross quadcopter shows an increase of 14 dB at 180° azimuth, and the plus quadcopter shows an even greater increase of 17 dB at 225° azimuth. These points are of interest because they are low noise points in hover. However, the directivity patterns diminish and eventually disappear in forward flight and thus the low noise locations exhibit the largest noise increase, which was also shown for the quadcopter noise in plane. Over the front half, the cross quadcopter noise increases by an average of 12.1 dB and the plus quadcopter by 10.1 dB, which are almost a full 10 dB greater than the noise increases seen in plane. The hexacopter does not show such a great increase in noise, although relative to in-plane the increase is more pronounced. The average increases by 2.4 dB when comparing hover and 60 knots. The octocopter also does not see as large an increase as the quadcopters, with the average noise increasing by 4.1 dB. To see the how strong the left-right noise bias is, we can compare the difference between the OASPL on the left and right. This is 0.44 dB for the cross quadcopter, 5.32 dB for the plus quadcopter, 3.05 dB for the hexacopter, and 7.41 for the octocopter. This again is due to the imbalance of outside advancing rotor blades on the left and right side of the vehicle.

Another metric that can be used for comparison is acoustic power radiated (PWL). Normalizing by the equivalent single rotor, this metric indicates how each multi-copter compares in terms of integrated noise, as shown in Table 3. Compared to the single rotor, all configurations radiate less acoustic power over the hemisphere for all the forward speed conditions, as shown by their negative numbers. Starting with 0 knots, the quad, both cross and plus, and octocopter are around a similar level of acoustic power radiated, while the hexacopter radiates slightly more. But, as they move into forward flight, it can be seen that the cross quadcopter starts to emit power quite similar to that of the single rotor, sticking to within a relative power of 0.16 dB, which is very small. Relative to the single rotor, the other

Table 3 – Power Radiated Relative to Equivalent Single Rotor

	0 Knots	15 Knots	30 Knots	60 Knots
Quadcopter Cross	-0.74 dB	-0.16 dB	-0.11 dB	-0.15 dB
Quadcopter Plus	-0.74 dB	-1.00 dB	-1.27 dB	-0.78 dB
Hexacopter	-0.30 dB	-0.64 dB	-1.72 dB	-1.22 dB
Octocopter	-0.70 dB	-1.39 dB	-2.44 dB	-1.98 dB

configurations emit less power moving into forward flight, reaching the minimum at 30 knots and seeing a slight relative increase at 60 knots. For the higher speeds, there is also a trend of less power being radiated for an increasing number of rotors.

3.3 Varying Disk Loading

Along with the effect of changing the number of rotors, the effect of changing the disk loading is examined. This is done for the plus orientated quadcopter, and the disk loadings examined are 3 lb/ft^2, 9 lb/ft^2, along with the baseline 6 lb/ft^2 that has was examined before. To change the disk loading, the tip Mach is varied, while holding the root pitch and all rotor geometric conditions constant. This results to a hover tip Mach of 0.36 for 3 lb/ft^2, 0.51 for 6 lb/ft^2, and 0.6 for 9 lb/ft^2.

Figure 13 shows the polar plots for the in-plane noise of the 3 lb/ft^2, 6 lb/ft^2, and 9 lb/ft^2 plus quadcopter for 0, 15, 30, and 60 knots forward flight speed. The most noticeable difference between disk loadings is the directivity in hover. The 3 lb/ft^2 case shows very deep lows at inter-boom locations, with a difference between minimum and maximum noise of 27.3 dB. This is compared to a difference of 10.4 dB for the 6 lb/ft^2 disk loading. The 9 lb/ft^2 hardly shows any real directivity of low noise at inter-booms and higher noise at rotor locations shown for the other two disk loadings. This difference in hover directivity intensity is caused by the lower tip Mach and is also discussed in Ref. 31. In summary, this is because the differences in the acoustic arrival times (due to rotor geometry and phasing) are higher for lower tip Mach numbers. Beyond differences in directivity, the 3 lb/ft^2 disk loading quadcopter shows a slightly higher increase in average noise, with an increase of 3.3 dB between 0 and 60 knots forward speed, compared to 1.8 dB for 6 lb/ft^2 and 1.9 dB for 9 lb/ft^2. This is because the 60 knots velocity corresponds to a higher advance ratio for the low disk loading/ low tip Mach number case, creating a higher relative increase in the tip Mach number.

Figure 14 gives similar polar plots for the 45° elevation angle. Unlike what was seen in-plane, the directivity patterns between all disk loadings are very comparable, with inter-boom lows observable at 135° and 225° azimuth and peak noise near rotor locations of 90°, 180°, and 270°. Similarly, this directivity is diminished once the vehicles enter forward flight for all disk loadings, as already discussed for the baseline case. There is a comparable left side bias that develops with forward speed (as discussed before), with the difference between noise at 90° and 270° azimuth being 4.4 dB for 3 lb/ft^2, 5.3 dB for 6 lb/ft^2, and 5.9 dB for 9 lb/ft^2 when considering 60 knots forward speed. The variance of this bias with disk loading is expected because the 60 knots velocity corresponds to a higher advance ratio for the low disk loading/ low tip Mach number case, and thus creates a higher asymmetry in the loading noise. The average noise increase observed is greater for the 3 lb/ft^2 than the other disk loadings, with an average increase of 10.8 dB compared to 9.8 dB for 6 lb/ft^2 and 7.4 dB for 9 lb/ft^2. Again, this is due to the higher advance ratio of the low disk loading case.

4. CONCLUSION

This study examines the acoustic behavior of manned-size, multi-rotor, eVTOL aircraft with four, six, and eight rotors (arranged in cross quadcopter, plus quadcopter, and vertex first hexacopter and octocopter) in forward flight speeds of 0, 15, 30, and 60 knots. The rotors are assumed to have collective pitch control, operating at specified RPM, allowing for the control of the phasing between rotors. Phasing between rotors was set to orthogonal, with all adjacent rotors being perfectly out of phase. To compare between multi-copters, the total disk area was preserved, thus the radius of the hexacopter and octocopter is reduced while the RPM was increased to match the tip Mach. An equivalent single rotor is also considered to allow comparisons to the multi-copters. The aerodynamic loads on the rotor blades are calculated using the Rensselaer Multicopter Analysis Code (RMAC) and these were provided as inputs to the acoustic propagation code PSU-WOPWOP to evaluate the acoustic pressure time history and OASPL in dB at specified observer locations. The acoustic pressure time history was then used to calculate the acoustic power radiated through an observer hemisphere. Form the simulations conducted, the following conclusions can be made:

1. The directivity patterns observed in-plane due to rotor phasing in hover (0 knots forward speed) are progressively diminished when operating in forward flight conditions. This is most clear on the nominal disk loading plus and cross quadcopter, where the directivity in-plane completely disappears at high forward flight speeds. This effect is less pronounced for the hexacopter and octocopter because the differences in the acoustic pathways are lower, and thus directivity is less affected at forward speeds.
2. As forward speed increases, loading noise becomes more dominant. This causes the regions of peak noise to move

towards below the vehicle where loading noise is directed for all configurations at speeds of 30 and 60 knots forward speed. The is also higher in the left (advancing) side for the plus quadcopter, hexacopter, and octocopter. This is due to the presence of advancing blades on the outside of the vehicle, which is a large source of loading noise.

3. The increase in noise at higher elevation angles is more pronounced for lower disk loadings. The 3 lb/ft^2 saw the greatest average increase in noise of 10.8 dB at 45° elevation, compared to 9.8 dB for 6 lb/ft^2 and 7.4 dB for 9 lb/ft^2. This is due to the lower disk loading quadcopter having a higher advanced ratio (due to the lower hover tip Mach number), thus increasing the effects of forward flight speeds.
4. The total acoustic radiated power is also evaluated and compared with the single rotor for all multi-copter configurations. The comparison shows that the acoustic power is decreasing as we increase the number of rotor and the forward speed. However, if A weighting is included the acoustic power increases for a higher number of rotors, with the forward speed reducing this effect.

ACKNOWLEDGEMENTS

This work was funded in part under the Army/Navy/NASA Vertical Lift Research Center of Excellence (VLRCOE) Program, grant number W911W61120012, with Dr. Mahendra Bhagwat as Technical Monitor.

REFERENCES

1. Holden, J., and Goel, N., "Fast-Forwarding to a Future of On-Demand Urban Air Transportation." UBER Elevate Whitepaper, October 2016, available at: https://www.uber.com/elevate.pdf [Accessed 10 Oct. 2019].
2. Swartz, K., "NASA Embraces Urban Air Mobility," Vertiflite Magazine, Jan-Feb 2019.
3. Schmitz, F., "The Challenges and Possibilities of a Truly Quiet Helicopter: 29th Alexander A. Nikolsky Honorary Lecture," *Journal of American Helicopter Society*, Vol. 61, No.4, 2016, pp. 1-33.
4. Zawodny, N. and Boyd, D. D., "Investigation of Rotor-Airframe Interaction Noise Associated with Small-Scale Rotary-Wing Unmanned Aircraft Systems," 73rd Annual Forum of the American Helicopter Society, Fort Worth, TX, 2017.
5. Pettingill, N. and Zawodny, N., "Identification and Prediction of Broadband Noise for a Small Quadcopter," 75th Annual Forum of the Vertical Flight Society, Philadelphia, PA, 2019.
6. Schiller, N., Pascioni, K., and Zawodny, N., "Tonal Noise Control using Rotor Phase Synchronization," 75th Annual Forum of the Vertical Flight Society, Philadelphia, PA, 2019.
7. Thurman, S. C., Zawodny, S. N., Baeder, D. J., "Computational Prediction of Broadband Noise from a Representative Small Unmanned Aerial System Rotor," 76th Annual Forum of the Vertical Flight Society, Virtual, 2020.
8. Pascioni, K. A., Rizzi, S. A., and Schiller, N.H., "Noise reduction potential of phase control for distributed propulsion vehicles," Paper AIAA 2019-1069, AIAA SciTech Forum and Exposition Proceedings, San Diego, CA, January 2019.
9. Tinney, C. and Sirohi, J., "Multirotor Drone Noise at Static Thrust," AIAA Journal, Vol. 56, No. 7, pp. 2816-2826, July 2018.
10. Tinney, C. and Valdez, J., "Acoustic Scaling for Small Rotors in Hover," 75th Annual Forum of the Vertical Flight Society, Philadelphia, PA, 2019.
11. Intaratep, N., Alexander, W., and Devenport, W., "Experimental Study of Quadcopter Acoustics and Performance at Static Thrust Conditions," *22nd AIAA/CEAS Aeroacoustics Conference*, Lyon, France, May 2016.
12. Quackenbush, T., Wachspress, D., Moretti, L., Barwey, D., Lewis, R., and Brentner, K., "Aeroacoustic Modeling of an eVTOL Slowed Rotor Winged Compound Aircraft," *75th Annual Forum of the Vertical Flight Society,* Philadelphia, PA, May 2019.
13. Jia, Z., and Lee, S., "Acoustic Analysis of Urban Air Mobility Quadrotor Aircraft," *Vertical Flight Society's Transformative Vertical Flight Forum*, San Jose, CA, Jan 21-23, 2020
14. Zawodny, N., Boyd, D. D., and Burley, C., "Acoustic Characterization and Prediction of Representative, Small-Scale Rotary-Wing Unmanned Aircraft System Components," *72nd Annual Forum of the American Helicopter Society,* West Palm Beach, FL, May 2016.
15. Lee, S., Shlesinger, I., "Coaxial Rotor Broadband Noise Prediction in Hover," 76th Annual Forum of the Vertical Flight Society, Virginia Beach, VA, 2020
16. Zawodny, N., Boyd, D. D., and Burley, C., "Acoustic Characterization and Prediction of Representative, Small-Scale Rotary-Wing Unmanned Aircraft System Components," *72nd Annual Forum of the American Helicopter Society,* West Palm Beach, FL, May 2016.
17. Jia, Z., and Lee, S., "Acoustic Analysis of Urban Air Mobility Quadrotor Aircraft," *Vertical Flight Society's Transformative Vertical Flight Forum*, San Jose, CA, Jan 21-23, 2020
18. Wachspress, D., Yu, M., and Brentner, K., "Rotor/Airframe Aeroacoustic Prediction for eVTOL UAM Aircraft," *75th Annual Forum of the Vertical Flight Society,* Philadelphia, PA, May 2019

19. Jia, Z., Lee, S., "Aeroacoustic Analysis of a Side-by-Side Hybrid VTOL Aircraft," 76th Annual Forum of the Vertical Flight Society, Virginia Beach, VA, 2020
20. Alvarez, J. E., Schenk, A., Critchfield, T., Ning, A., "Rotor-on-Rotor Aeroacoustic Interactions of Multirotor in Hover," 76th Annual Forum of the Vertical Flight Society, Virginia Beach, VA, 2020
21. Jacobellis, G., Singh, R., Johnson, C., Sirohi, J., McDonald, R., "Experimental and Computational Investigation of Stacked Rotor Acoustics in Hover," 76th Annual Forum of the Vertical Flight Society, Virginia Beach, VA, 2020
22. Walter, A., McKay, M., Niemiec, R., Gandhi, F., and Ivler, C., "Handling Qualities Based Assessment of Scalability for Variable-RPM Electric Multi-Rotor Aircraft," *75th Annual Forum of the Vertical Flight Society*, Philadelphia, PA, May 2019.
23. Bahr, M., McKay, M., Niemiec, R., and Gandhi, F., "Performance and Handling Qualities Assessment of Large Variable-RPM Multi-Rotor Aircraft for Urban Air Mobility," *76th Annual Forum of the Vertical Flight Society,* Montreal, Canada, May 2020.
24. Walter, A., McKay, M., Niemiec, R., Gandhi, F., Ivler, C., "Disturbance Rejection and Handling Qualities of Fixed-Pitch, Variable-RPM Quadcopters with Increasing Rotor Diameter," *76th Annual Forum of the Vertical Flight Society,* Montreal, Canada, May 2020.
25. Niemiec, R., Gandhi, F., Lopez, M., and Tischler, M., "System Identification and Handling Qualities Predictions of an eVTOL Urban Air Mobility Aircraft Using Modern Flight Control Methods," *76th Annual Forum of the Vertical Flight Society,* Montreal, Canada, May 2020.
26. https://evtol.news/2020/01/15/joby-aviation-unveils-s4/, accessed February 21, 2020.
27. Kopyt, N., Niemiec, R., and Gandhi, F., "Quadcopter Rotor Phasing for Minimization of Aircraft Vibratory Loads," *Vertical Flight Society's Transformative Vertical Flight Forum*, San Jose, CA, Jan 21-23, 2020.
28. Kopyt, N., Niemiec, R., and Gandhi, F., "Optimal Rotor Phasing for Multicopter Vibratory Load Minimization," *76th Annual Forum of the Vertical Flight Society,* Montreal, Canada, May 2020.
29. Niemiec, R. and Gandhi, F., "Development and Validation of the Rensslaer Multicopter Analysis Code (RMAC): A Physics-Based Comprehensive Modeling Tool," *75th Annual Forum of the Vertical Flight Society,* Philadelphia, PA, May 2019.
30. Brentner, K., Bres, G. A., and Perez, G., "Maneuvering Rotorcraft Noise Prediction: A New Code for a New Problem," *AHS Aerodynamics, Acoustics, and Test and Evaluation Technical Specialist Meeting,* San Fransisco, CA, Jan. 2002.
31. Smith, B., Niemic, R., Gandhi, F., "A Comparison of Multicopter Noise Characteristics with Increasing Number of Rotors" 76th Annual Forum of the Vertical Flight Society, Virtual, 2020